THE JOURNAL OF PHYSICAL CHEMISTRY LETTERS
A JOURNAL OF THE AMERICAN CHEMICAL SOCIETY

pubs.acs.org/JPCL

Letter

Magnetic Circular Dichroism of Porphyrinoid Silver Complexes: Evidence of the Electronic Structure Inversion upon Protonation of the N-Confused Core

Dustin E. Nevonen, Jenna C. Wagner, Christian Brückner,* Christopher J. Ziegler,* and Victor N. Nemykin*

Cite This: *J. Phys. Chem. Lett.* 2023, 14, 7382−7388

Read Online

ACCESS | Metrics & More | Article Recommendations | Supporting Information

ABSTRACT: We report a systematic investigation of a series of Ag(II) and Ag(III) complexes of porphyrins and their analogues using UV−vis magnetic circular dichroism (MCD) spectroscopies and theoretical calculations. Ag(II) and Ag(III) octaethyl- and tetraarylporphyrins show the usual sign sequence in the Q-band region (i.e., negative to positive intensities with increasing energy) of their MCD spectra, indicative of the ΔHOMO > ΔLUMO relationship (ΔHOMO is the energy difference between Michl's *a* and *s* orbitals, and ΔLUMO is the energy difference between Michl's *-a* and *-s* pair of MOs). In contrast, Ag(II) complexes of *β,β′*-pyrrole-modified porphyrins (with an effective chlorin-type *π*-system) and Ag(III) corroles have sign reverse features in the MCD spectra of their Q-band region (ΔHOMO < ΔLUMO relationships). The Ag(III) complex of N-confused porphyrin shows the ΔHOMO > ΔLUMO relationship in the neutral state and the ΔHOMO < ΔLUMO relationship in the protonated form.

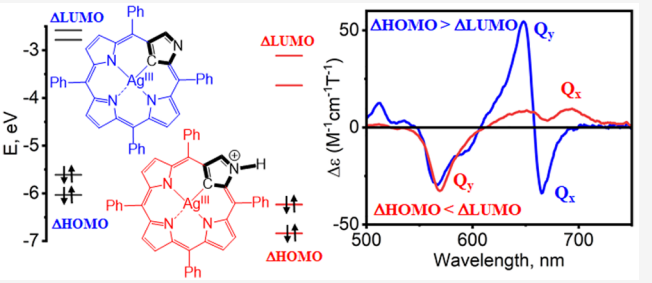

Silver porphyrins have been known for decades since the initial report of the EPR spectrum of silver deuteroporphyrin IX dimethyl ester in 1961.[1] One of the unique features of these systems is the accessibility of both Ag(II) and Ag(III) oxidation states in which the silver ion remains in the square-planar porphyrin coordination environment.[2−10] Since their discovery, silver porphyrins have been investigated, e.g., for electrocatalytic and biomedical applications.[11−14] The silver complexes of porphyrin isomers and analogues, such as N-confused porphyrins,[15−17] core-modified porphyrins,[18,19] and corroles,[20−28] have received significantly less attention.[29−34]

Modification of the porphyrin skeleton alters the electronic structure of the porphyrin isomers and analogues; we have been investigating these systems for the past decade using magnetic circular dichroism (MCD) spectroscopy.[35−42] MCD spectroscopy is a powerful method to allow the unambiguous assignment of the relative energy differences in the porphyrin-centered frontier orbitals. In particular, when asymmetry is incorporated into the porphyrin macrocycle, an inversion of the magnitude of the ΔHOMO versus the ΔLUMO is observed, as described by Gouterman's four-orbital[43−45] and Michl's perimeter models.[46−49] In these models, ΔHOMO[46−49] is the energy difference between the Gouterman's porphyrin-centered a_{1u} ("*a*" orbital in Michl's perimeter model) and a_{2u} ("*s*" orbital in Michl's perimeter model) orbitals in the standard D_{4h} point group notation, while ΔLUMO[46−49] is the energy difference between the Gouterman's porphyrin-centered $e_{g(x)}$ and $e_{g(y)}$ orbitals ("*-a*" and "*-s*" orbitals in Michl's perimeter model) in the standard D_{4h} point group notation. For the sake of clarity, we will continue to use this standard notation for all low-symmetry porphyrinoids discussed in this paper. In standard 4-fold symmetric main-group or transition-metal porphyrins, the ΔLUMO is zero (the $e_{g(x)}$ and $e_{g(y)}$ orbitals are degenerate because the effective symmetry of these systems is D_{4h} or C_{4v}), and the ΔHOMO is nonzero, which results in the typical ΔHOMO > ΔLUMO relationship. In lower-symmetry porphyrins and analogues such as the chlorins and bacteriochlorins, the LUMO and LUMO+1 are nondegenerate. In many cases, a ΔHOMO < ΔLUMO energy relationship is observed; it is expressed as the so-called reversed sequence of the readily observed MCD *B* terms in the Q-band region.[35,36,40−42]

The square-planar geometry in both Ag(II) and Ag(III) porphyrinoids provides a unique chance to investigate the influence of the parent or modified porphyrin skeleton on the electronic structure of Gouterman's and Michl's frontier

Received: June 16, 2023
Accepted: August 7, 2023
Published: August 11, 2023

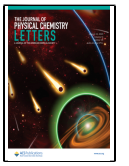

https://doi.org/10.1021/acs.jpclett.3c01658
J. Phys. Chem. Lett. 2023, 14, 7382−7388

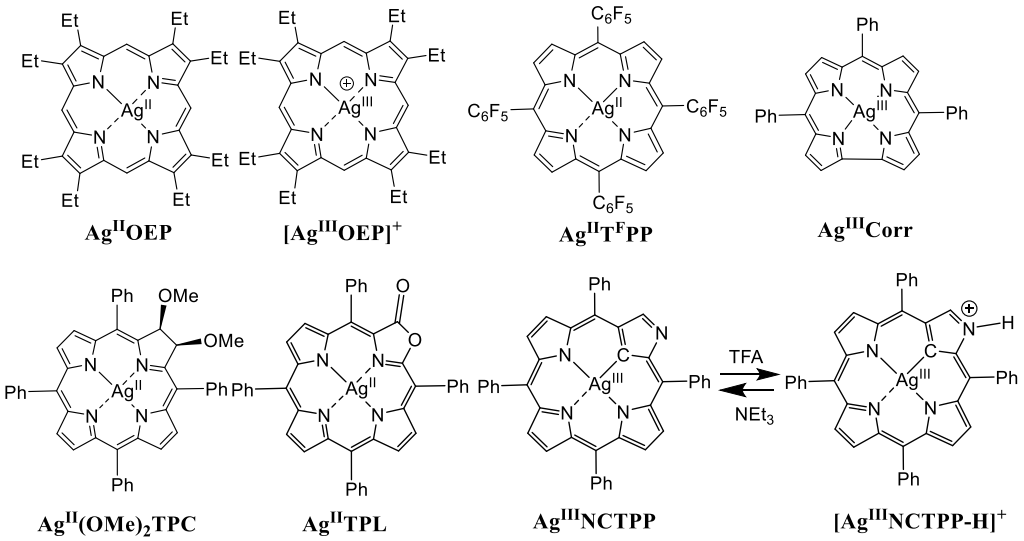

Figure 1. Structures of Ag(II) and Ag(III) porphyrinoids studied in this work.

orbitals. Indeed, Au(III) porphyrinoids can be either tetra- or pentacoordinated (which affects the energies of frontier MOs), while polarization ability of Cu(II) and Cu(III) in porphyrinoids is significantly higher than in the respective silver analogues. To the best of our knowledge, there also has been no systematic study of the MCD spectra of "regular" Ag(II) and Ag(III) porphyrins. Indeed, the MCD spectra of such systems were only reported by McCaffery for $Ag^{II}OEP$[50] and Furuta and coauthors for a single neutral Ag(III) doubly N-confused porphyrin.[51]

Thus, we compare here the MCD spectra and electronic structures of a series of literature-known Ag(II) and Ag(III) complexes of porphyrins, chlorin, N-confused porphyrin, skeletal-modified porphyrins, and corrole (Figure 1) in order to elucidate the influence of backbone modification on the electronic structure of these systems. All of these complexes have a porphyrinoid ligand in its neutral state coupled with Ag(II) or Ag(III) centers.[18]

The UV−vis and MCD spectra of $Ag^{II}OEP$ and $[Ag^{III}OEP]^+$ complexes are typical of the OEP-based metal compounds with effective D_{4h} symmetry (Figure 2A,B).[50] In particular, four clear MCD Faraday *A* terms at ∼555, ∼522, ∼407, and ∼333 nm are observed for these compounds. The slightly higher-energy shift of doubly degenerate Q_{0-0} (∼555 nm) and Q_{0-1} (∼522 nm) bands for the $[Ag^{III}OEP]^+$ complex is reflective of the stabilization of its HOMO as well as LUMO and LUMO+1 orbitals, upon oxidation of the silver center; this finding is further discussed in the DFT section below. It is also worth noting that the *A* term associated with the Q_{0-0} transition in the MCD spectrum of the $[Ag^{III}OEP]^+$ complex is significantly stronger than the *A* term observed for the Soret band at ∼407 nm.

The MCD spectrum of the $Ag^{II}T^FPP$ complex is also reflective of its effective 4-fold symmetry and is dominated by the MCD *A* term associated with the Soret band centered at 419 nm (Figure 2C). The Q_{0-0} (568 nm) and Q_{0-1} (535 nm) bands are also represented by two MCD *A* terms of significantly reduced (compared with the Soret band) intensities. The presence of MCD *A* terms in all of these silver complexes confirms the degeneracy of the porphyrin-centered Gouterman's e_g pair of MOs.[43−45]

In contrast, the MCD spectrum of the $Ag^{III}Corr$ complex is reflective of its lower symmetry (Figure 2D). Corrole is a ring contracted porphyrinoid with a direct pyrrole−pyrrole link. This porphyrinoid is trianionic and stabilizes silver in the +3 oxidation state. In particular, the Q_x (585 nm) and Q_y (559 nm) bands in its UV−vis spectrum are associated with two MCD *B* terms at 582 and 558 nm, respectively. This observation of positive to negative (in ascending energy) MCD *B* terms is reflective of ΔHOMO < ΔLUMO relationship in this complex. In the Soret band region, an MCD pseudo-*A* term centered at 425 nm is associated with the Soret band at 422 nm observed in its UV−vis spectrum. Again, two closely spaced MCD *B* terms have a positive-to-negative (in ascending energy) sequence. The overall shape of the MCD spectrum of $Ag^{III}Corr$ is characteristic of the $M^{III}Corr$ complexes with *meso*-tetraryl-substituted pattern reported thus far.[35,36,52,53]

The silver chlorin ($Ag^{II}(OMe)_2TPC$) and silver chlorin-like chromophores ($Ag^{II}TPL$)[19,54] also have positive-to-negative (in ascending energy) MCD *B* terms, which is reflective of the ΔHOMO < ΔLUMO relationship in these complexes. In both of these systems, the porphyrin skeleton is modified at one of the pyrrole units that breaks the overall symmetry of the ring. In the case of the $Ag^{II}(OMe)_2TPC$ complex, Q_x (598 nm) and Q_y (574 nm) bands in its UV−vis spectrum are associated with two MCD *B* terms observed at 599 and 572 nm, respectively, and are well-separated from each other (Figure 2E). This is not the case for the lactone-containing $Ag^{II}TPL$ complex, in which positive and negative MCD *B* terms are closely spaced (595 and 577 nm) with both signals associated with the absorption band observed at 591 nm (Figure 2F). This observation correlates well with the DFT calculations discussed below, which are indicative of a much smaller LUMO−LUMO+1 energy gap in the $Ag^{II}TPL$ complex compared to that in the $Ag^{II}(OMe)_2TPC$ complex. The Soret band in the UV−vis spectra of both chlorine-type complexes is associated with MCD pseudo-*A* terms. However, the closely spaced *B* terms in this region exhibit an opposite sign sequence. Indeed, it is positive-to-negative (in ascending energy) in the $Ag^{II}(OMe)_2TPC$ complex and negative-to-positive (in ascending energy) in the $Ag^{II}TPL$ complex.

https://doi.org/10.1021/acs.jpclett.3c01658
J. Phys. Chem. Lett. 2023, 14, 7382−7388

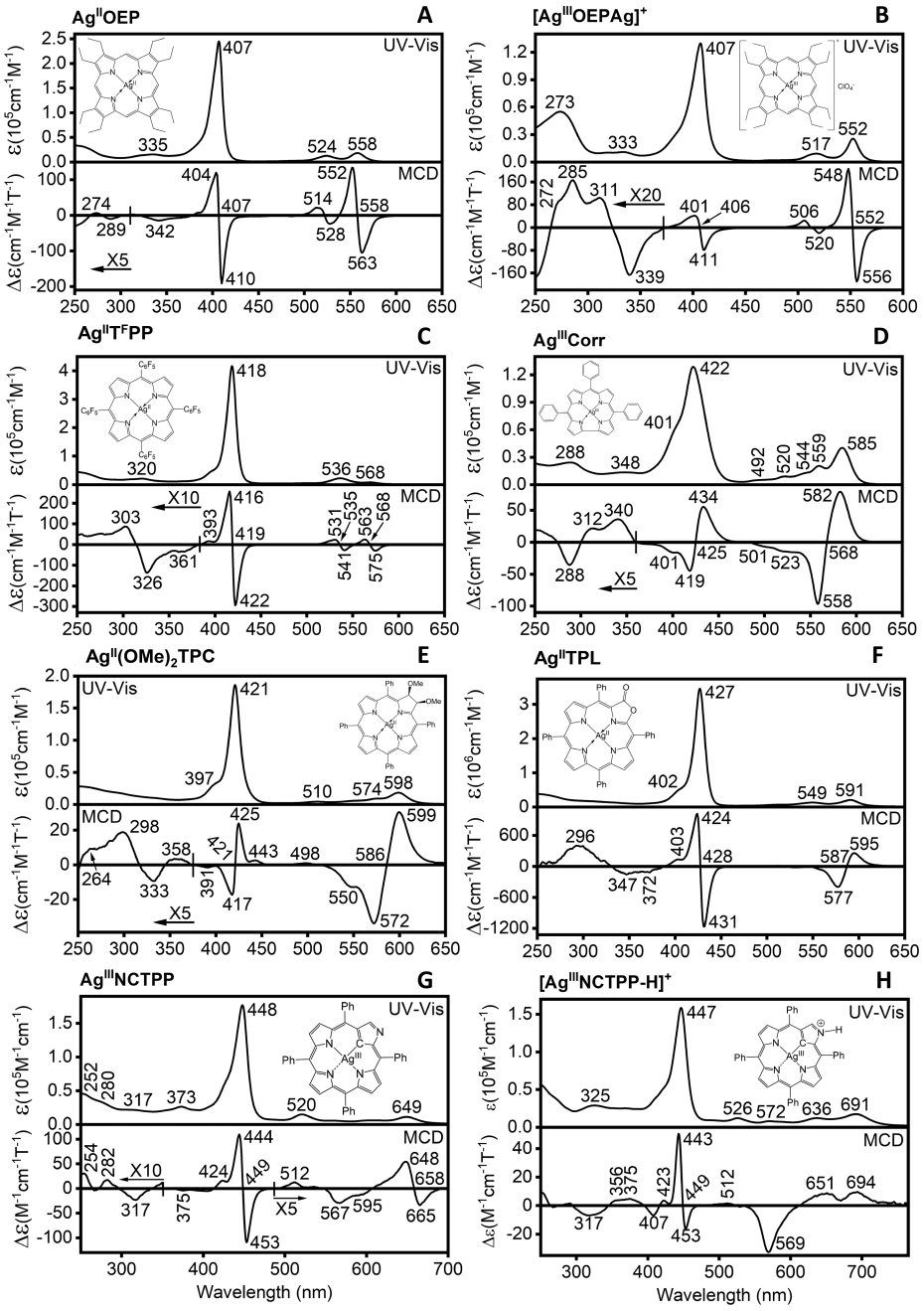

Figure 2. UV−vis and MCD spectra (CH_2Cl_2) of the Ag(II) and Ag(III) complexes.

The most interesting MCD spectra were observed for Ag(III) N-confused porphyrin Ag^{III}NCTPP in its neutral and protonated forms (Figure 2G,H). Indeed, neutral Ag^{III}NCTPP has a single intense band in the Q-band region at 649 nm. However, the MCD spectrum of this compound possesses two closely spaced *B* terms at 648 and 665 nm. The negative-to-positive sign sequence is indicative of a ΔHOMO > ΔLUMO relationship in this compound, similar to the other symmetric silver porphyrins. The UV region is dominated by a strong MCD pseudo-*A* term centered at 449 nm, which correlates well with the UV−vis Soret band for this compound. However, once the outer nitrogen atom is transformed from an imine to amine type via (reversible) protonation, the MCD spectrum of the resulting $[Ag^{III}NCTPP\text{-}H]^+$ complex changes significantly (Figure 3). First, two MCD *B* terms at 694 and 651 nm have

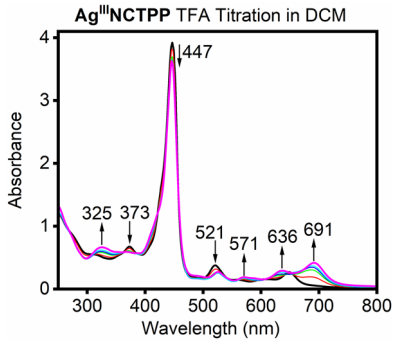

Figure 3. Transformation of Ag^{III}NCTPP to $[Ag^{III}NCTPP\text{-}H]^+$ upon adding of 0−1 equiv of trifluoroacetic acid (TFA) in CH_2Cl_2.

https://doi.org/10.1021/acs.jpclett.3c01658
J. Phys. Chem. Lett. 2023, 14, 7382−7388

positive amplitudes, while the intense *B* term with a negative amplitude is observed at 569 nm (Figure 2H). We assign the $Q_{0-0(x)}$ transition to the absorption at 691 nm, the $Q_{0-1(x)}$ band to the absorption at 651 nm, and the $Q_{0-0(y)}$ band to the absorption observed at 569 nm. Thus, simple protonation of the outer nitrogen atom in the Ag^{III}NCTPP complex leads to an inversion of the ΔHOMO < ΔLUMO relationship in the $[Ag^{III}NCTPP\text{-}H]^+$ complex. The Soret band region of the $[Ag^{III}NCTPP\text{-}H]^+$ complex is again dominated by the MCD pseudo-*A* term. However, its negative *B* term component intensity is significantly reduced.

We previously reported a similar electronic structural change in the transition-metal N-confused porphyrins for complexes with divalent cations that have pyrrole-type outer NH protons in their neutral forms.[37,38] Those complexes have a ΔHOMO < ΔLUMO relationship, which can be reversed upon deprotonation of the outer NH bond. Overall, it therefore seems that although the central metal in porphyrins can affect the energies of the Q and Soret bands, the relative magnitudes of ΔHOMO and ΔLUMO are dictated by the structure of the porphyrinoid chromophore. The typical porphyrins and N-confused porphyrins with imine-type outer nitrogen atom have a ΔHOMO > ΔLUMO relationship, while corroles, chlorin-type porphyrinoids, and N-confused porphyrins with amine type outer NH units exhibit a ΔHOMO < ΔLUMO relationship.

To further elucidate the electronic structures and excited-state properties in silver porphyrinoids, we conducted DFT and TDDFT calculations on these systems using hybrid TPSSh,[55] M06,[56] and long-range separated wB97X[57] exchange-correlation functionals. All functionals provided close electronic structures and vertical excitation energies for the target compounds. The M06-predicted energy diagram for all silver compounds is shown in Figures 4 and S1, while

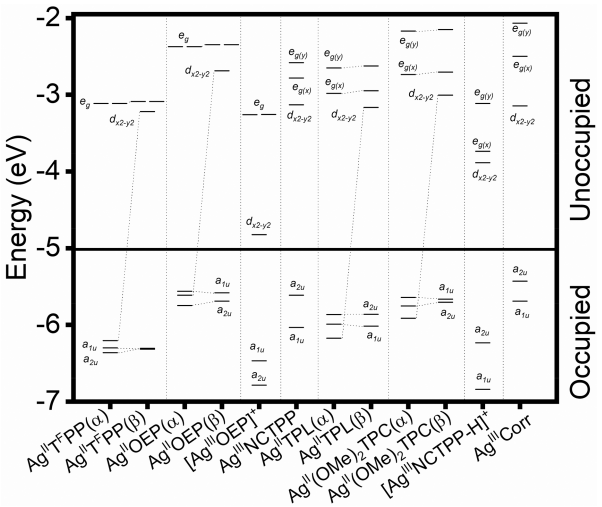

Figure 4. DFT-predicted (M06) partial energy diagram for Ag(II) and Ag(III) complexes.

representative frontier orbital images are pictured in Figures 5 and S2. In the case of all Ag(III) complexes and Ag(II) complexes, DFT predicts that the LUMO or *β*-LUMO has silver-centered $d_{x^2-y^2}$ character, respectively with the LUMO+1 and LUMO+2 being Gouterman's porphyrinoid-based $e_{g(x)}$ (Michl's *-a*) and $e_{g(y)}$ (Michl's *-s*) MOs.[43−45] The HOMO and HOMO−1 in Ag(III) systems are the porphyrinoid-based

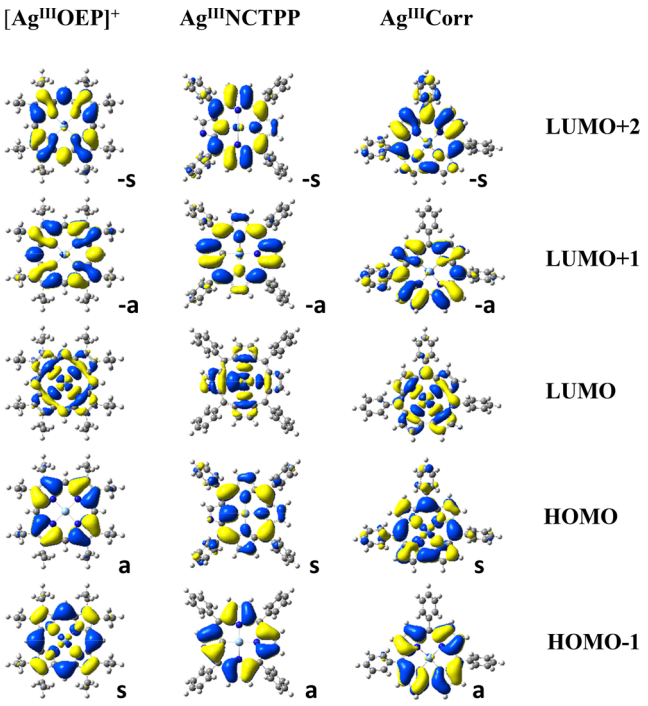

Figure 5. Representative examples of DFT-predicted (M06) porphyrin-centered Gouterman's type frontier orbitals (the isosurface value is 0.02) and silver-centered $d_{x^2-y^2}$ orbitals in Ag(II) and Ag(III) systems. Michl's orbital labels are used.

Gouterman's a_{2u} (Michl's *s*) and a_{1u} (Michl's *a*) orbitals.[43−45] This is also true for the *β*-set of MOs in Ag(II) systems. The *α*-set frontier MOs in Ag(II) complexes have closely spaced $d_{x^2-y^2}$, a_{1u}, and a_{2u} orbitals. As expected, the OEP-based systems and chlorin-type complexes have a_{1u} MOs at energies higher than those of a_{2u} MOs, while the opposite is predicted for *meso*-tetraaryl-containing complexes. More importantly, DFT calculations predict the ΔHOMO > ΔLUMO relationships for the Ag^{II}OEP, Ag^{III}OEP, $Ag^{II}T^FPP$, and Ag^{III}NCTPP complexes, and the opposite relationship occurs for the remaining compounds, which is in excellent agreement with the observed MCD data. The flip of the electronic structure between Ag^{III}NCTPP and $[Ag^{III}NCTPP\text{-}H]^+$ complexes is similar to that observed in the Ni(II) N-confused porphyrins.[37,38] These observations can be explained on a basis of the perturbation theory discussed earlier by us for singly N-confused porphyrins[37,38] and by Kobayashi's group for double N-confused porphyrins.[58] Indeed, the transformation of the amine NH ring in the N-confused porphyrin core to imine one should result in destabilization of Gouterman's a_{2u} and one of e_g orbitals (*s* and *−s* orbitals in Michl's notation)[46−49] and stabilization of Gouterman's a_{1u} and another e_g orbitals (Michl's *a* and *−a* MOs).

The TDDFT-predicted UV−vis spectra of all target silver complexes are shown in Figures 6 and S3. UV−vis spectra of all three "standard" porphyrins (Ag^{II}OEP, $[Ag^{III}OEP]^+$, and $Ag^{II}T^FPP$) can be easily described using Gouterman's four-orbital model,[43−45] which implies that both the Q and Soret bands are dominated by a_{1u}, $a_{2u} \rightarrow e_g$ single-electron transitions. TDDFT also predicts correctly that the energy gap between the Q_x and Q_y bands in the Ag^{II}TPL complex is smaller than that in the $Ag^{II}(OMe)_2$TPC and Ag^{III}Corr complexes. Following their electronic structures, the Q_x band is dominated by the $a_{2u} \rightarrow e_{g(x)}$ or $e_{g(y)}$ single-electron

https://doi.org/10.1021/acs.jpclett.3c01658
J. Phys. Chem. Lett. 2023, 14, 7382−7388

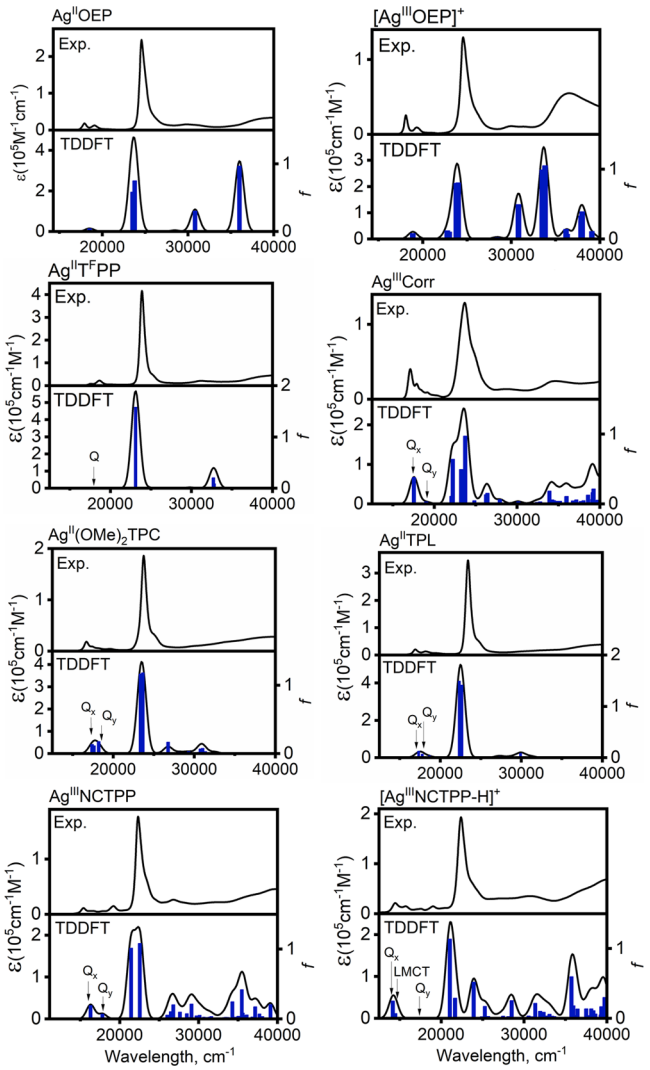

Figure 6. Comparison between the experimental and TDDFT-predicted (M06; 0.1 eV bandwidth) UV−vis spectra of Ag(II) and Ag(III) complexes.

excitations for Ag^{II}TPL and Ag^{III}Corr complexes, while the $a_{1u} \rightarrow e_{g(x)}$ or $e_{g(y)}$ single-electron excitation is responsible for the appearance of the Q_x band in the $Ag^{II}(OMe)_2$TPC complex. In the case of the Ag^{II}NCTTP complex, the Q_x and Q_y bands are dominated by the HOMO (a_{2u}) → LUMO+1 and HOMO (a_{2u}) → LUMO+2 single-electron excitations (LUMO in this complex has $d_{x^2-y^2}$ character). Both bands are predicted to have a significant intensity, in agreement with the experiment although their splitting is slightly overestimated in TDDFT calculations. In the case of the protonated $[Ag^{III}NCTPP\text{-}H]^+$ complex, the Q_x band is dominated by the HOMO (a_{2u}) → LUMO+1 ($e_{g(x)}$) single-electron excitation and predicted to have a relatively high intensity. However, the Q_y band, which is dominated by the HOMO (a_{2u}) → LUMO+2 ($e_{g(y)}$) single-electron excitation, is predicted to have a very low intensity independent of the exchange-correlation functional used. In agreement with the experimental data, a larger Q_x-Q_y energy gap is predicted for the $[Ag^{III}NCTPP\text{-}H]^+$ complex compared to that in Ag^{III}NCTPP. Interestingly, an additional band of relatively high intensity was predicted with the energy close to the Q_x band in the $[Ag^{III}NCTPP\text{-}H]^+$ complex (Figure 6). This band is dominated by the HOMO−1 (a_{1u}) → LUMO ($d_{x^2-y^2}$) single-electron excitation and has significant ligand-to-metal charge-transfer (LMCT) character. Overall, TDDFT calculations correlate well with the experimental data and are indicative of the operational Gouterman's four-orbital model in description of the Ag(II) and Ag(III) porphyrinoids.

In conclusion, we demonstrated that the UV−vis and MCD spectra as signatures for the electronic structures of Ag(II) and Ag(III) porphyrinoids are dominated by the structures of the chromophore. Porphyrin complexes have a ΔHOMO > ΔLUMO relationship, while the less symmetric chlorin-like and corrole complexes have a ΔHOMO < ΔLUMO relationship. The protonation of the external nitrogen atom in N-confused Ag^{III}NCTPP complex changes the electronic structure from the ΔHOMO > ΔLUMO to the rarer ΔHOMO < ΔLUMO system. DFT-calculated ΔHOMO and ΔLUMO energy gaps were found to be consistent with the observed MCD sign sequences in the context of Michl's perimeter model. TDDFT calculations also provided good agreement between theory and experiment and are indicative of the validity of Gouterman's four-orbital model in the description of the Ag(II) and Ag(III) porphyrinoids studied.

■ ASSOCIATED CONTENT

Supporting Information

The Supporting Information is available free of charge at https://pubs.acs.org/doi/10.1021/acs.jpclett.3c01658.

Experimental part and additional DFT and TDDFT information (PDF)

■ AUTHOR INFORMATION

Corresponding Authors

Victor N. Nemykin − *Department of Chemistry, University of Tennessee, Knoxville Tennessee 37996, United States;* orcid.org/0000-0003-4345-0848; Email: vnemykin@utk.edu

Christopher J. Ziegler − *Department of Chemistry, University of Akron, Akron, Ohio 44325-3601, United States;* orcid.org/0000-0002-0142-5161; Email: ziegler@uakron.edu

Christian Brückner − *Department of Chemistry, University of Connecticut, Storrs, Connecticut 06269-3060, United States;* orcid.org/0000-0002-1560-7345; Email: c.bruckner@uconn.edu

Authors

Dustin E. Nevonen − *Department of Chemistry, University of Tennessee, Knoxville Tennessee 37996, United States*

Jenna C. Wagner − *Department of Chemistry, University of Akron, Akron, Ohio 44325-3601, United States*

Complete contact information is available at: https://pubs.acs.org/10.1021/acs.jpclett.3c01658

Notes

The authors declare no competing financial interest.

■ ACKNOWLEDGMENTS

C.J.Z. acknowledges the University of Akron for support of this research. C.B. acknowledges the support from the NSF (CHE-1800361). Generous support from the NSF (CHE-2153081), Minnesota Supercomputing Institute, and the University of Tennessee to V.N. is greatly appreciated.

REFERENCES

(1) Kneubuhl, F. K.; Koski, W. S.; Caughey, W. S. An electron spin resonance study of silver porphyrin. *J. Am. Chem. Soc.* **1961**, *83*, 1607−1609.

(2) Araki, C.; Yamamoto, K.; Tokunaga, C. Effect of γ-rays on the nickel, zinc, and silver chelates of $\alpha,\beta,\gamma,\delta$-tetraphenylporphine. *Rikagaku Kenkyusho Hokoku* **1964**, *40*, 45−49.

(3) Manoharan, P. T.; Rogers, M. T. E.S.R. study of copper(II) and silver(II) tetraphenylporphyrin. *Electron Spin Resonance Metal Complexes*; Yen, T. F., Ed.; 1969; pp 143−173.

(4) Kadish, K.; Davis, D. G.; Fuhrhop, J. H. Unusual oxidation states of metalloporphyrins. Octaethylporphinatosilver(III) perchlorate. *Angew. Chem., Int. Ed.* **1972**, *11*, 1014−1016.

(5) Schneider, M. L. Crystal structure of a (tetraphenylporphine)-silver-tetraphenylporphine molecular solid solution. *J. Chem. Soc., Dalton Trans.* **1972**, 1093−1096.

(6) Karweik, D.; Winograd, N.; Davis, D. G.; Kadish, K. M. X-ray photoelectron spectroscopic studies of silver(III) octaethylporphyrin. *J. Am. Chem. Soc.* **1974**, *96*, 591−592.

(7) Antipas, A.; Dolphin, D.; Gouterman, M.; Johnson, E. C. Porphyrins. 38. Redox potentials, charge transfer transitions, and emission of copper, silver, and gold complexes. *J. Am. Chem. Soc.* **1978**, *100*, 7705−7709.

(8) Dzhagarov, B. M.; Timinskii, Yu. V.; Chirvonyi, V. S.; Gurinovich, G. P. Study of short-lived excited states of complexes of porphyrins with iron(III), cobalt(II) and silver(II) using picosecond flash photolysis. *Doklady Akademii Nauk SSSR* **1979**, *247*, 728−731.

(9) Chirvonyi, V. S.; Dzhagarov, B. M.; Timinskii, Yu. V.; Gurinovich, G. P. Picosecond flash photolysis of nickel(II) and silver(II) porphyrins. *Chem. Phys. Lett.* **1980**, *70*, 79−83.

(10) Kadish, K. M.; Lin, X. Q.; Ding, J. Q.; Wu, Y. T.; Araullo, C. A reinvestigation of silver porphyrin electrochemistry. Reactions of silver(III), silver(II), and silver(I). *Inorg. Chem.* **1986**, *25*, 3236−3242.

(11) Becker, J. Y.; Vainas, B.; Eger, R.; Kaufman, L. Electrocatalytic reduction of carbon dioxide to oxalate by silver(II) and palladium(II) porphyrins. *J. Chem. Soc., Chem. Commun.* **1985**, 1471−1472.

(12) Guterres, K. B.; Rossi, G. G.; de Campos, M. M. A.; Moreira, K. S.; Burgo, T. A. L.; Iglesias, B. A. Nanomolar effective report of tetracationic silver(II) porphyrins against non-tuberculous mycobacteria in antimicrobial photodynamic approaches. *Photodiagnosis Photodynamic Therapy* **2022**, *38*, 102770.

(13) Cao, M.; Wang, S.; Hu, J.-H.; Lu, B.-H.; Wang, Q.-Y.; Zang, S.-Q. Silver Cluster-Porphyrin-Assembled Materials as Advanced Bioprotective Materials for Combating Superbacteria. *Adv. Sci.* **2022**, *9*, 2103721.

(14) He, J.; Yin, Y.; Shao, Y.; Zhang, W.; Lin, Y.; Qian, X.; Ren, Q. Synthesis of a Rare Water-Soluble Silver(II)/Porphyrin and Its Multifunctional Therapeutic Effect on Methicillin-Resistant Staphylococcus aureus. *Molecules* **2022**, *27*, 6009.

(15) Araki, K.; Winnischofer, H.; Toma, H. E.; Maeda, H.; Osuka, A.; Furuta, H. Acid-Base and Spectroelectrochemical Properties of Doubly N-Confused Porphyrins. *Inorg. Chem.* **2001**, *40*, 2020−2025.

(16) Furuta, H.; Ogawa, T.; Uwatoko, Y.; Araki, K. N-Confused Tetraphenylporphyrin-Silver(III) Complex. *Inorg. Chem.* **1999**, *38*, 2676−2682.

(17) Sumra, I.; Irfan, M.; He, H.; Zhang, Y.; Hao, F.; Lin, J.; Osuka, A.; Zeng, Z.; Jiang, H.-W. Regioselective Carbon-Halogen Bond Formation in the Reaction of Ag(III) N-Confused Porphyrin Complex with HCl or HBr. *Eur. J. Org. Chem.* **2021**, *2021*, 4440−4443.

(18) Brückner, C. The silver complexes of porphyrins, corroles, and carbaporphyrins: Silver in the oxidation states II and III. *J. Chem. Educ.* **2004**, *81*, 1665−1669.

(19) McCarthy, J. R.; Melfi, P. J.; Capetta, S. H.; Brückner, C. Use of Ag(II) as a removable template in porphyrin chemistry: diol cleavage products of [meso-tetraphenyl-2,3-cis-diolchlorinato]silver(II). *Tetrahedron* **2003**, *59*, 9137−9146.

(20) Sinha, W.; Sommer, M. G.; Deibel, N.; Ehret, F.; Sarkar, B.; Kar, S. Silver Corrole Complexes: Unusual Oxidation States and Near-IR-Absorbing Dyes. *Chem.—Eur. J.* **2014**, *20*, 15920−15932.

(21) Yadav, I.; Osterloh, W. R.; Kadish, K. M.; Sankar, M. Synthesis, Spectral, Redox, and Sensing Studies of β-Dicyanovinyl-Appended Corroles and Their Metal Complexes. *Inorg. Chem.* **2023**, *62*, 7738−7752.

(22) Lemon, C. M.; Powers, D. C.; Huynh, M.; Maher, A. G.; Phillips, A. A.; Tripet, B. P.; Nocera, D. G. Ag(III)···Ag(III) Argentophilic Interaction in a Cofacial Corrole Dyad. *Inorg. Chem.* **2023**, *62*, 3−17.

(23) Ueta, K.; Nakai, A.; Tanaka, T.; Osuka, A. Synthesis of 8,12-Dibromocorrole and Its Transformation to Antiaromatic 8,10-Fused Iminoisocorrole with a Polarized Resonance Contribution. *Chem.—Asian J.* **2021**, *16*, 2253−2256.

(24) Stefanelli, M.; Ricci, A.; Chiarini, M.; Lo Sterzo, C.; Berionni Berna, B.; Pomarico, G.; Sabuzi, F.; Galloni, P.; Fronczek, F. R.; Smith, K. M.; Wang, L.; Ou, Z.; Kadish, K. M.; Paolesse, R. β-Arylethynyl substituted silver corrole complexes. *Dalton Trans* **2019**, *48*, 13589−13598.

(25) Patra, B.; Sobottka, S.; Sinha, W.; Sarkar, B.; Kar, S. Isovalent AgIII/AgIII, AgII/AgII, Mixed-Valent AgII/AgIII, and Corrolato-Based Mixed-Valency in β,β'-Linked [Bis{corrolato-silver}]n Complexes. *Chem.—Eur. J.* **2017**, *23*, 13858−13863.

(26) Stefanelli, M.; Mastroianni, M.; Nardis, S.; Licoccia, S.; Fronczek, F. R.; Smith, K. M.; Zhu, W.; Ou, Z.; Kadish, K. M.; Paolesse, R. Functionalization of corroles: the nitration reaction. *Inorg. Chem.* **2007**, *46*, 10791−10799.

(27) Ding, T.; Aleman, E. A.; Modarelli, D. A.; Ziegler, C. J. Photophysical Properties of a Series of Free-Base Corroles. *J. Phys. Chem. A* **2005**, *109*, 7411−7417.

(28) Ding, T.; Harvey, J. D.; Ziegler, C. J. N-H tautomerization in triaryl corroles. *J. Porphyrins Phthalocyanines* **2005**, *9*, 22−27.

(29) Lash, T. D. Metal complexes of carbaporphyrinoid systems. *Chem.—Asian J.* **2014**, *9*, 682−705.

(30) Lash, T. D.; Colby, D. A.; Szczepura, L. F. New riches in carbaporphyrin chemistry: Silver and gold organometallic complexes of benzocarbaporphyrins. *Inorg. Chem.* **2004**, *43*, 5258−5267.

(31) Muckey, M. A.; Szczepura, L. F.; Ferrence, G. M.; Lash, T. D. Silver(iii) carbaporphyrins: The first organometallic complexes of true carbaporphyrins. *Inorg. Chem.* **2002**, *41*, 4840−4842.

(32) Pokharel, K.; Ferrence, G. M.; Lash, T. D. Late transition metal complexes of oxypyriporphyrin and the platinum(ii) complex of oxybenziporphyrin. *J. Porphyrins Phthalocyanines* **2017**, *21*, 493−501.

(33) Lash, T. D. Carbaporphyrinoid systems. *Chem. Rev.* **2017**, *117*, 2313−2446.

(34) Lash, T. D.; Miyake, K.; Xu, L.; Ferrence, G. M. Synthesis of a series of aromatic benziporphyrins and heteroanalogues via tripyrrane-like intermediates derived from resorcinol and 2-methylresorcinol. *J. Org. Chem.* **2011**, *76*, 6295−6308.

(35) Rhoda, H. M.; Crandall, L. A.; Geier, G. R., III; Ziegler, C. J.; Nemykin, V. N. Combined MCD/DFT/TDDFT Study of the Electronic Structure of Axially Pyridine Coordinated Metallocorroles. *Inorg. Chem.* **2015**, *54*, 4652−4662.

(36) Ziegler, C. J.; Sabin, J. R.; Geier, G. R.; Nemykin, V. N. The first TDDFT and MCD studies of free base triarylcorroles: A closer look into solvent-dependent UV-visible absorption. *Chem. Commun.* **2012**, *48*, 4743−4745.

(37) Doble, S.; Osinski, A. J.; Holland, S. M.; Fisher, J. M.; Geier, G. R.; Belosludov, R. V.; Ziegler, C. J.; Nemykin, V. N. Magnetic Circular Dichroism of Transition-Metal Complexes of Perfluorophenyl-N-Confused Porphyrins: Inverting Electronic Structure through a Proton. *J. Phys. Chem. A* **2017**, *121*, 3689−3698.

(38) Sripothongnak, S.; Ziegler, C. J.; Dahlby, M. R.; Nemykin, V. N. Controllable and Reversible Inversion of the Electronic Structure in Nickel N-Confused Porphyrin: A Case When MCD Matters. *Inorg. Chem.* **2011**, *50*, 6902−6909.

https://doi.org/10.1021/acs.jpclett.3c01658
J. Phys. Chem. Lett. 2023, 14, 7382−7388

(39) Ziegler, C. J.; Erickson, N. R.; Dahlby, M. R.; Nemykin, V. N. Magnetic Circular Dichroism Spectroscopy of N-Confused Porphyrin and Its Ionized Forms. *J. Phys. Chem. A* **2013**, *117*, 11499−11508.
(40) Rhoda, H. M.; Akhigbe, J.; Ogikubo, J.; Sabin, J. R.; Ziegler, C. J.; Brückner, C.; Nemykin, V. N. Magnetic Circular Dichroism Spectroscopy of meso-Tetraphenylporphyrin-Derived Hydroporphyrins and Pyrrole-Modified Porphyrins. *J. Phys. Chem. A* **2016**, *120*, 5805−5815.
(41) Brückner, C.; Chaudhri, N.; Nevonen, D. E.; Bhattacharya, S.; Graf, A.; Kaesmann, E.; Li, R.; Guberman-Pfeffer, M. J.; Mani, T.; Nimthong-Roldan, A.; Zeller, M.; Chauvet, A. A. P.; Nemykin, V. Structural and Photophysical Characterization of All Five Constitutional Isomers of the Octaethyl-*β*,*β*'-dioxo-bacterio- and -isobacteriochlorin Series. *Chem.—Eur. J.* **2021**, *27*, 16189−16203.
(42) Dorazio, S. J.; Vogel, A.; Dechert, S.; Nevonen, D. E.; Nemykin, V. N.; Brückner, C.; Meyer, F. Siamese-Twin Porphyrin Goes Platinum: Group 10 Monometallic, Homobimetallic, and Heterobimetallic Complexes. *Inorg. Chem.* **2020**, *59*, 7290−7305.
(43) Gouterman, M. J. *The Porphyrins*; Dolphin, D., Ed.; Academic Press: New York, 1978; Vol. *III*, pp 1−654.
(44) Gouterman, M. Spectra of Porphyrins. *J. Mol. Spectrosc.* **1961**, *6*, 138−163.
(45) Seybold, P. G.; Gouterman, M. Porphyrins. *J. Mol. Spectrosc.* **1969**, *31*, 1−13.
(46) Waluk, J.; Michl, J. Perimeter Model and Magnetic Circular Dichroism of Porphyrin Analogs. *J. Org. Chem.* **1991**, *56*, 2729−2735.
(47) Michl, J. Magnetic Circular Dichroism of Cyclic *π*-Electron Systems. 1. Algebraic Solution of the Perimeter Model for the A and B Terms of High-Symmetry Systems with a (4N + 2)-Electron [N]annulene Perimeter. *J. Am. Chem. Soc.* **1978**, *100*, 6801−6811.
(48) Michl, J. Magnetic Circular Dichroism of Cyclic *π*-Electron Systems. 2. Algebraic Solution of the Perimeter Model for the B Terms of Systems with a (4N + 2)-Electron [N]annulene Perimeter. *J. Am. Chem. Soc.* **1978**, *100*, 6812−6818.
(49) Michl, J. Magnetic Circular Dichroism of Cyclic *π*-Electron Systems. 3. Classification of Cyclic.pi. Chromophores with a (4N + 2)-Electron [N]annulene Perimeter and General Rules for Substituent Effects on the MCD Spectra of Soft Chromophores. *J. Am. Chem. Soc.* **1978**, *100*, 6819−6824.
(50) Gale, R.; McCaffery, A. J.; Rowe, M. D. Magnetic circular dichroism and absorption spectra of the porphyrins. I. *J. Chem. Soc., Dalton Trans.* **1972**, 596−604.
(51) Yan, J.; Yang, Y.; Ishida, M.; Mori, S.; Zhang, B.; Feng, Y.; Furuta, H. Organometallic Group 11 (CuIII, AgIII, AuIII) Complexes of a trans-Doubly N-Confused Porphyrin: An "Expanded Imidazole" Structural Motif. *Chem.—Eur. J.* **2017**, *23*, 11375−11384.
(52) Liang, X.; Mack, J.; Zheng, L.-M.; Shen, Z.; Kobayashi, N. Phosphorus(V)-Corrole: Synthesis, Spectroscopic Properties, Theoretical Calculations, and Potential Utility for in Vivo Applications in Living Cells. *Inorg. Chem.* **2014**, *53*, 2797−2802.
(53) Cai, F.; Xia, F.; Guo, Y.; Zhu, W.; Fu, B.; Liang, X.; Wang, S.; Cai, Z.; Xu, H. Off-on-off" type of selectively pH-sensing 8-hydroxyquinoline-substituted gallium(III) corrole. *New J. Chem.* **2019**, *43*, 18012−18017.
(54) Brückner, C.; Ogikubo, J.; McCarthy, J. R.; Akhigbe, J.; Hyland, M. A.; Daddario, P.; Worlinsky, J. L.; Zeller, M.; Engle, J. T.; Ziegler, C. J.; Ranaghan, M. J.; Sandberg, M. N.; Birge, R. R. Oxazolochlorins. 6. Meso-arylporpholactones and their reduction products. *J. Org. Chem.* **2012**, *77*, 6480−6494.
(55) Tao, J. M.; Perdew, J. P.; Staroverov, V. N.; Scuseria, G. E. Climbing the Density Functional Ladder: Nonempirical Meta-Generalized Gradient Approximation Designed for Molecules and Solids. *Phys. Rev. Lett.* **2003**, *91*, 146401.
(56) Zhao, Y.; Truhlar, D. G. The M06 Suite of Density Functionals for Main Group Thermochemistry, Thermochemical Kinetics, Noncovalent Interactions, Excited States, and Transition Elements: Two New Functionals and Systematic Testing of Four M06 Functionals and Twelve Other Functionals. *Theor. Chem. Acc.* **2008**, *120*, 215−241.
(57) Chai, J. D.; Head-Gordon, M. Systematic Optimization of Long-Range Corrected Hybrid Density Functionals. *J. Chem. Phys.* **2008**, *128*, 084106.
(58) Muranaka, A.; Homma, S.; Maeda, H.; Furuta, H.; Kobayashi, N. Detection of Unusual ΔHOMO<ΔLUMO Relationship in Tetrapyrrolic Cis- and Trans-Doubly N-Confused Porphyrins. *Chem. Phys. Lett.* **2008**, *460*, 495−498.

https://doi.org/10.1021/acs.jpclett.3c01658
J. Phys. Chem. Lett. 2023, 14, 7382−7388